Video Article

An In Vivo Duo-color Method for Imaging Vascular Dynamics Following Contusive Spinal Cord Injury

Chen Chen[1,2], Yi Ping Zhang[3], Yan Sun[1,4], Wenhui Xiong[1], Lisa B. E. Shields[3], Christopher B. Shields[3,5], Xiaoming Jin[1], Xiao-Ming Xu[1]

[1]Spinal Cord and Brain Injury Research Group, Stark Neurosciences Research Institute, and Department of Neurological Surgery, Indiana University School of Medicine

[2]Program in Medical Neuroscience, Stark Neurosciences Research Institute, Indiana University School of Medicine

[3]Norton Neuroscience Institute, Norton Healthcare

[4]Department of Human Anatomy & Histoembryology, School of Basic Medical Sciences, Fudan University

[5]Department of Neurological Surgery, University of Louisville School of Medicine

Correspondence to: Xiao-Ming Xu at xu26@iupui.edu

Abstract

Spinal cord injury (SCI) causes significant vascular disruption at the site of injury. Vascular pathology occurs immediately after SCI and continues throughout the acute injury phase. In fact, endothelial cells appear to be the first to die after a contusive SCI. The early vascular events, including increased permeability of the blood-spinal cord barrier (BSCB), induce vasogenic edema and contribute to detrimental secondary injury events caused by complex injury mechanisms. Targeting the vascular disruption, therefore, could be a key strategy to reduce secondary injury cascades that contribute to histological and functional impairments after SCI. Previous studies were mostly performed on postmortem samples and were unable to capture the dynamic changes of the vascular network. In this study, we have developed an *in vivo* duo-color two-photon imaging method to monitor acute vascular dynamic changes following contusive SCI. This approach allows detecting blood flow, vessel diameter, and other vascular pathologies at various sites of the same rat pre- and post-injury. Overall, this method provides an excellent venue for investigating vascular dynamics.

Video Link

The video component of this article can be found at https://www.jove.com/video/56565/

Introduction

Traumatic spinal cord injury (SCI) is a common injury leading to impairment of the motor, sensory, and autonomous function. According to the National Spinal Cord Injury Statistical Center (NSCISC) in 2016, approximately 282,000 persons were affected while 69% of them were mainly due to traffic accidents or falls[1]. These patients often require intensive care; however, no effective treatment is currently available. Therefore, new effective strategies towards SCI are urgently needed.

SCI is mainly divided into two phases: primary injury and secondary injury. The primary injury comprises the physical insult causing hemorrhagic necrosis at the site of impact[2], followed by a series of secondary injury events, such as inflammation, cell apoptosis, and demyelination of remaining axons, that progressively lead to the expansion of morphological and functional deficits[3,4,5,6]. Hemorrhage is the first visible sign of injury, indicating an immediate vascular disruption in the acute phase of SCI[7,8]. A neuroprotective strategy aimed at reducing the early vascular damage could improve patients' recovery, but this requires a better understanding of the pathophysiological mechanism of early post-injury vascular events.

Despite previous studies using various methods to study spinal cord vasculature, significant limitations remain. The most shared disadvantage is studying only postmortem samples, for example, hydrogen clearance[9], autoradiography[10], microangiogram[8], vascular corrosion casts[11], and immunohistochemistry[12,13]. Although Laser Doppler Flowmetry provides noninvasive real-time monitoring of spinal cord blood flow[14], it is unable to differentiate between vascular systems and detect vascular morphological changes. Dynamic Contrast-enhanced MRI (DCE-MRI) is also noninvasive, but it generates low-resolution images and requires an expensive infrastructure[15].

Although *in vivo* imaging using 2-photon laser scanning microscopy (2P-LSM) has been developed for studying vasodynamics in the cortex[16,17,18], a limited number of studies have demonstrated vascular changes following a SCI. Tang et al. have shown changes in blood flow at the edge of the lesion site in a hemisection model[19], but imaging after a contusive injury is more challenging for two reasons. First, a traditional glass optical window over the injury site would not sustain the mechanical impact and remain functional for imaging. Second, the leakage of tracer into the parenchyma due to hemorrhage creates difficulty with post-injury imaging.

Here we present a novel duo-color imaging method, which allows imaging the same individual vessels at pre- and post-injury time points. In addition, it provides a temporal-spatial profile of vascular dynamic changes following a contusive SCI. It also has the potential for imaging at multiple post-injury time points. This protocol can be directly applied to transgenic animals to study neurovascular interaction.

Protocol

All surgical and animal handling procedures were performed as approved under the Guide for the Care and Use of Laboratory Animals (National Research Council) and the Guidelines of the Indiana University School of Medicine Institutional Animal Care and Use Committee.

1. Surgical Preparation

1. Sterilize all surgical tools including the spine stabilizer. Clean the surgical table and all the surrounding area with 70% ethanol. For preparation of the non-survival surgical procedure, place a clean surgical pad on the top of a 37 °C heating pad.
2. Use six week old Sprague Dawley (SD) rat for this study. Weigh and anesthetize the rat with an intraperitoneal injection of ketamine (87.7 mg/kg) and xylazine (12.3 mg/kg) mixture. Confirm proper stage of anesthesia when the animal ceases to respond to a toe pinch stimulus. Subcutaneously inject 0.01-0.05 mg/kg Buprenorphine and 5mg/kg Carprofen prior to surgery.
3. Shave the rat in 2 areas: the cervical spine region on the back and the neck region on the breast side. Swab the skin areas with betadine surgical scrub and 70% alcohol wipes. Apply eye ointment to prevent dry eye during surgery. Place the animal in a supine position on the clean surgical pad.

2. External Jugular Vein Catheterization

1. Locate the external jugular vein by finding the pulse point near the collarbone, and cut with a pair of small spring scissors to make a vertical incision on the spot,which is the cross-point of 3 anatomical points: caudal ramus of right mandible, greater tubercle of humerus and manubrium (**Figure 1A**). Isolate the vessel using spring scissors and fine forceps. Tie the distal end with 1 sterile surgical suture line(**Figure 1C**)[20].
2. Prepare one 1-mL syringe filled with saline and connected with a specialized catheter made from a 21-gauge needle (**Figure 1B**). Make a small incision using a pair of micro scissors on the vessel and slide the catheter into the vessel.
    1. Secure the needle by tying both the proximal and distal end (**Figure 1C**). The specialized catheter is made from a 21-gauge needle. Grind the tip flat and weld with a 2-mm piece of tip cut off from another 21-gauge needle. This can prevent the catheter from slipping outside.
       Note: A small amount of blood flowing into the needle indicates that the needle has entered a blood vessel successfully.

3. Spine Stabilization and C5-C7 Laminectomy

1. Place the animal in a prone position. Cut the skin along the midline with a No. 15 scalpel blade at the desired spinal levels. Dissect the muscle layers from the 5th to 7th cervical vertebrae (C5-C7) bilaterally to expose the lateral facets (**Figure 2A**)[21].
   Note: Locate the second thoracic vertebra (T2) by finding the spike between the scapulae. Count upward from the T2 vertebra to find the C7 vertebra[21,22,23,24].
2. Stabilize the spine of the rat using a modified stabilizing apparatus. Make a slit on both sides of the lateral vertebral bone. Slide the stainless-steel arms underneath the exposed transverse process facets and tighten the screws to secure stability (**Figure 2B**).
3. Carefully remove the C5-C7 laminae (laminectomy, **Figure 2C**).
4. Place a small piece of saline-soaked gelfoam on top of the exposed dura mater to keep it moisturized (**Figure 2D**).

4. Installation of Two-photon (2P) Imaging Window

1. Stuff small pieces of gelfoam into the gap between muscles and vertebral bones, also stuff a thin line of gelfoam between spinal cord and vertebral bones, then use tissue adhesive glue to seal the surrounding muscle-bone area. Wait 5 min for complete dryness (**Figure 2E**).
   Note: This step effectively prevents future bleeding into the window and leakiness of immersion solutions.
2. Prepare 4% agar with ddH$_2$O in a microwave. After the agar is completely dissolved, wait until it returns to a touchable temperature. Fill a 1-mL sterile syringe with agar solution and pipe it onto the edge of the window to build a wall (**Figure 2E**). The solution solidifies quickly and remains flexible to allow the lens or objective to move freely.
3. When ready for imaging, remove the gelfoam and place immersion fluid inside the window for 2P imaging (**Figure 2F**). Transfer the stabilized animal inside the 2-photon microscope dark chamber and place the 2P imaging window directly under the lens. Lower the lens carefully into the imaging window.

5. Injection of First Fluorescent Dye and Baseline Imaging

1. Prepare 0.5 mL of Rhodamine B isothiocyanate-Dextran (4 mg/mL average molecular weight ~70kDa) in saline. Fill a 1-mL sterile syringe with the solution and connect the syringe to the previously installed catheter.
   Note: Preparing the fluorescent dye solution before use is recommended.
2. Inject the first dye by depressing the syringe very slowly (**Figure 3B**). First, use the eyepiece to identify the area of interest. Use a charge coupled device (CCD) camera to acquire a bright-field image of the surface blood vessel patterns at lower magnification as a landmark image. Switch to laser scanning mode and then open the 2P imaging software for collecting both images and line-scan data.

3. Select the proper 2P laser excitation wavelength, power, and fluorescent channel (red channel for first dye) to match with the fluorophores used in the imaged tissue, and then perform *in vivo* imaging (**Figure 3E**). Keep the animal on a heating pad during the whole process.

6. C7 Contusive Injury using LISA device

1. Perform a C7 midline contusion injury using a Louisville Injury System Apparatus (LISA) device according to a previously established protocol[25,26].
    1. In brief, place the animal on the LISA stage following calibration. After selecting a zero-point setting and adjusting tissue displacement (0.800 mm in this case), click the "Run Experiment" button of the software to trigger the impactor release and create the injury.
    2. After the injury, place another small piece of saline-soaked gelfoam on top of the exposed dura mater to keep it moisturized.
2. Repeat step 4.3 and re-perform *in vivo* imaging on the same area visible with the previously injected red dye (**Figure 3C** &F).
3. Transfer the animal back to the surgical table and keep the animal sedated with appropriate anesthesia following the IACUC-IUSM protocol.

7. Injection of Second Fluorescent Dye and Post-injury Imaging

1. Prepare 0.5 mL of Fluorescein isothiocyanate-dextran (4 mg/mL, average molecular weight ~70 kDa) in saline same as in 5.1. Fill the solution in a 1-mL sterile syringe and connect with the previously installed catheter.
2. Transfer the stabilized animal back inside the 2P microscope dark chamber and re-image the same area with the red channel for the first dye and the green channel for the second dye (Figures 3D & G).
3. At the end of imaging, release the rat from the spinal stabilization device and clean the agar wall.

8. Animal Sacrifice

1. After imaging, sacrifice the rat following the transcardial perfusion protocol[27]. Collect the spinal cord samples and fix them in 4% PFA.

9. Offline Data Analysis: Quantification of Vessel Diameters

1. Transfer the image files to a workstation for off-line analysis.
2. Open ImageJ and select "file" and then choose previously saved raw data and open the associated single image file (**Figure 4B**).
3. Calibrate the image by selecting "Analyze" followed by "Set Scale" (**Figure 4C**). The value placed in "Distance in pixels" is calculated using the equation displayed in **Figure 4A**. The calibration of 2-photon optical lens determines the default value in the equation. The value of "opticalZoom" is found in Excel Extensible Markup Languagefile (XML file) associated with the single image file (**Figure 4B**).
4. Draw a line perpendicular to the long axis of the vessel (**Figure 4D$_1$** & **E$_1$**) and select "Analyze" followed by "Measure". The measurement of vessel diameter is displayed in the result window (**Figure 4D$_2$** & **E$_2$**). Repeat 3 times across the vessel to acquire the average value.

10. Offline Data Analysis: Quantification of red blood cell (RBC) Velocity

1. Transfer the line-scan files to the workstation for analysis.
2. Start the ImageJ software and select "file" and then choose previously saved raw data and open all associated line-scan files with the extension name ".ome".
3. Open "Image" and select "Stacks" followed by "images to stack". Convert all OME files into a single image stack TIFF file.
4. Start Matlab software and click "Open", select "LSPIV_parallel.m" code file. Note: Matlab code for LS-PIV can be downloaded at https://sourceforge.net/projects/lspivsupplement/files/[18]
5. Select the following orders: "Run">"Change Folder">"artery". Choose the image stack TIFF file generated in **10.3**.
6. Type "Y" and press Enter.
7. Place a cursor on the left and right side of the image respectively, and the program starts to process the data.
8. At the end of the program, enter 2 values to calculate the final read: "pixel_meter conversion value", and "scan-time conversion value". Both can be found in the XML file associated with line-scan data. The final value is expressed as the mean and standard deviation of velocity in the units of millimeter per second (mm/s).

Representative Results

The method is able to monitor *in vivo* dynamic spinal vascular changes in individual vessels pre- and post-traumatic SCI. First, a catheter is installed via the external jugular vein to provide access for subsequent fluorescent dye injections (**Figure 1A-C**, **Figure 3**). In the second step, a specialized apparatus is used to stabilize the exposed C5-C7 (**Figure 1D-F**, **Figure 2A-B**). This stabilization step can eliminate breathing artifacts and provide steady imaging. Following laminectomy (**Figure 2C**), the next step is the installation of 2P imaging window over C5-C7 (**Figure 2D-F**). Minimizing peripheral tissue bleeding around the spinal imaging window is critical for successful vascular imaging. The following step is to inject rhodamine-dextran fluorescent dye (Red) via the aforementioned catheter to landmark and map the vascular network as the baseline (**Figure 3A-B**, **E**). After C7 midline contusive injury with moderate severity, FITC-dextran (Green) is introduced at desired post-injury time points (**Figure 3A** & **D**). The beauty of the duo-color method is that one can still detect the vascular structure using the second dye when the first dye has already leaked out into parenchyma due to injury (**Figure 3G**).

During the imaging session, it is advisable to keep the animal on a heating pad to maintain body core temperature after anesthesia induction.

Using our duo-color method, the diameter and red blood cell velocity (RBC velocity) of individual vessels can be measured and calculated. For diameter, one can use ImageJ to measure the vessel at its largest diameter for 3 repeats after calibration (**Figure 4**). For velocity, line-scan images are measured using Matlab program (MATLAB R2013a) to calculate the RBC velocity (**Figure 5**)[18]. Based on the morphology, blood flow velocity, and vessel diameter, the vessels can be classified into 2 categories: artery and vein (See Table 1).
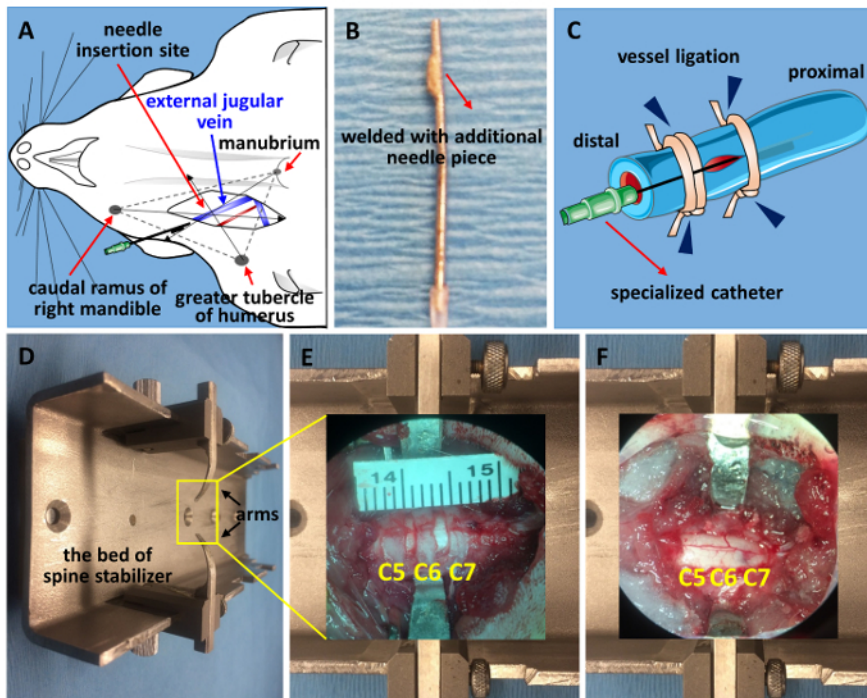

Figure 1. Jugular vein catheterization and spine stabilization.
(A) A schematic drawing for locating the external jugular vein. **(B)** The specialized catheter made from a 21-gauge needle. The tip was ground flat and welded with a piece of 2 millimeter tip cut off from another 21-gauge needle. **(C)** A schematic diagram of catheterization. The distal end is ligated first, followed by proximal catheter stabilization, ending with fastening the needle along with the vessel (vessel ligation, blue arrowheads). **(D)** An image of the modified spine stabilizer. A C5-C7 window prior to laminectomy **(E)** and after laminectomy and contusive SCI **(F)** is displayed. Please click here to view a larger version of this figure.
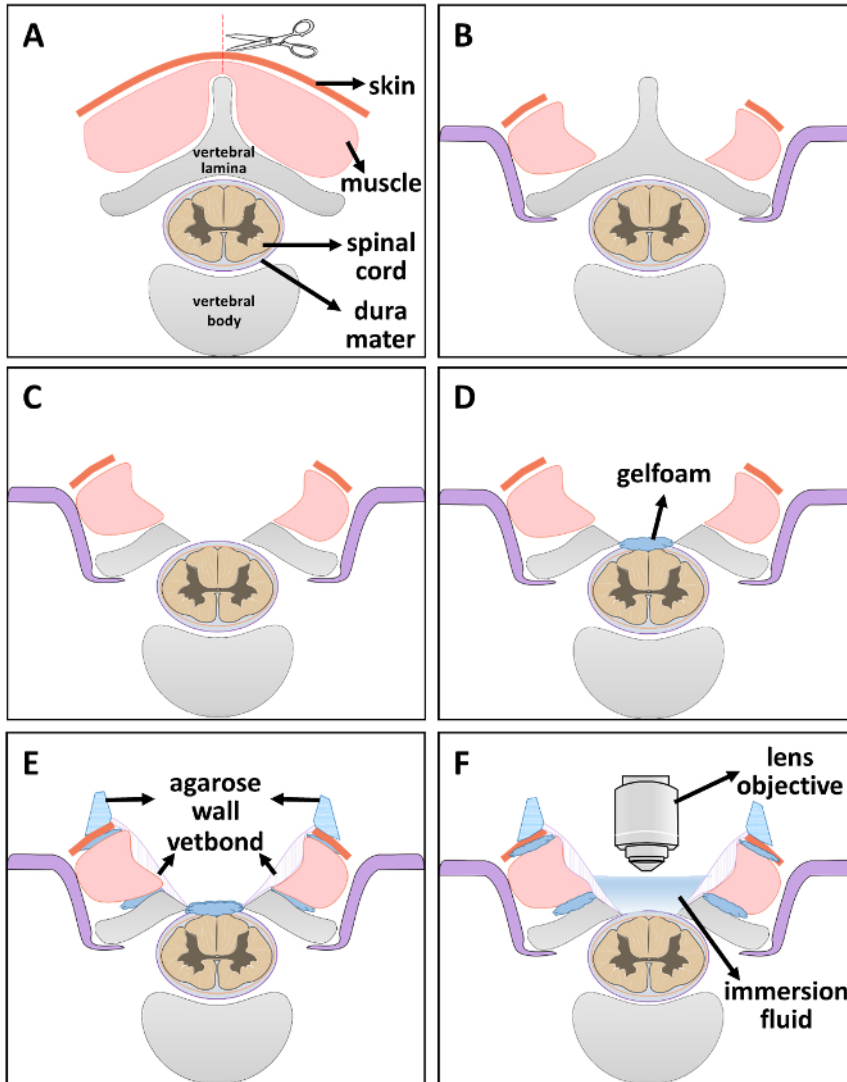
Figure 2. Schematic diagram of optic window installation step-by-step.
(A) Step 1: expose the vertebra by cutting skin and muscle along the midline. **(B)** Step 2: spine stabilization. **(C)** Step 3: laminectomy. **(D)** Step 4: maintain the moisture of spinal cord by placing a piece of saline-soaked gelfoam. **(E)** Step 5: seal the gaps with sterile gelfoam and vetbond. After drying, a layer of agar wall is built on the edge of the window. **(F)** Step 6: when ready for imaging, remove the gelfoam and place immersion fluid inside 2P imaging window. Please click here to view a larger version of this figure.
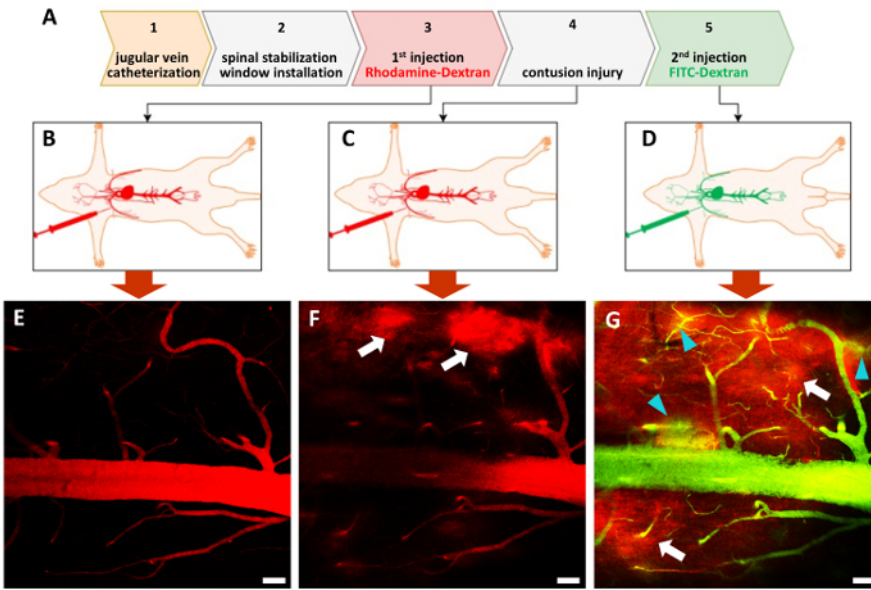
Figure 3. The *in vivo* duo-color method procedure step-by-step.
The whole procedure consists of 5 steps **(A)**. Following Step 1 and Step 2, a pair of dextran tracers with a size of approximate 70 KDa are injected in sequence to label the spinal cord vasculature before **(B** and **C)** and after contusive SCI **(D)**. **(E)-(G)** representative 2P images display the spinal cord vasculature at Step 3 through Step 5. White arrows point to first-wave red dye leaking areas (**F** and **G**), turquoise arrowheads display second-wave green dye leakage **(G)**. Scale bar = 50 µm. Please click here to view a larger version of this figure.
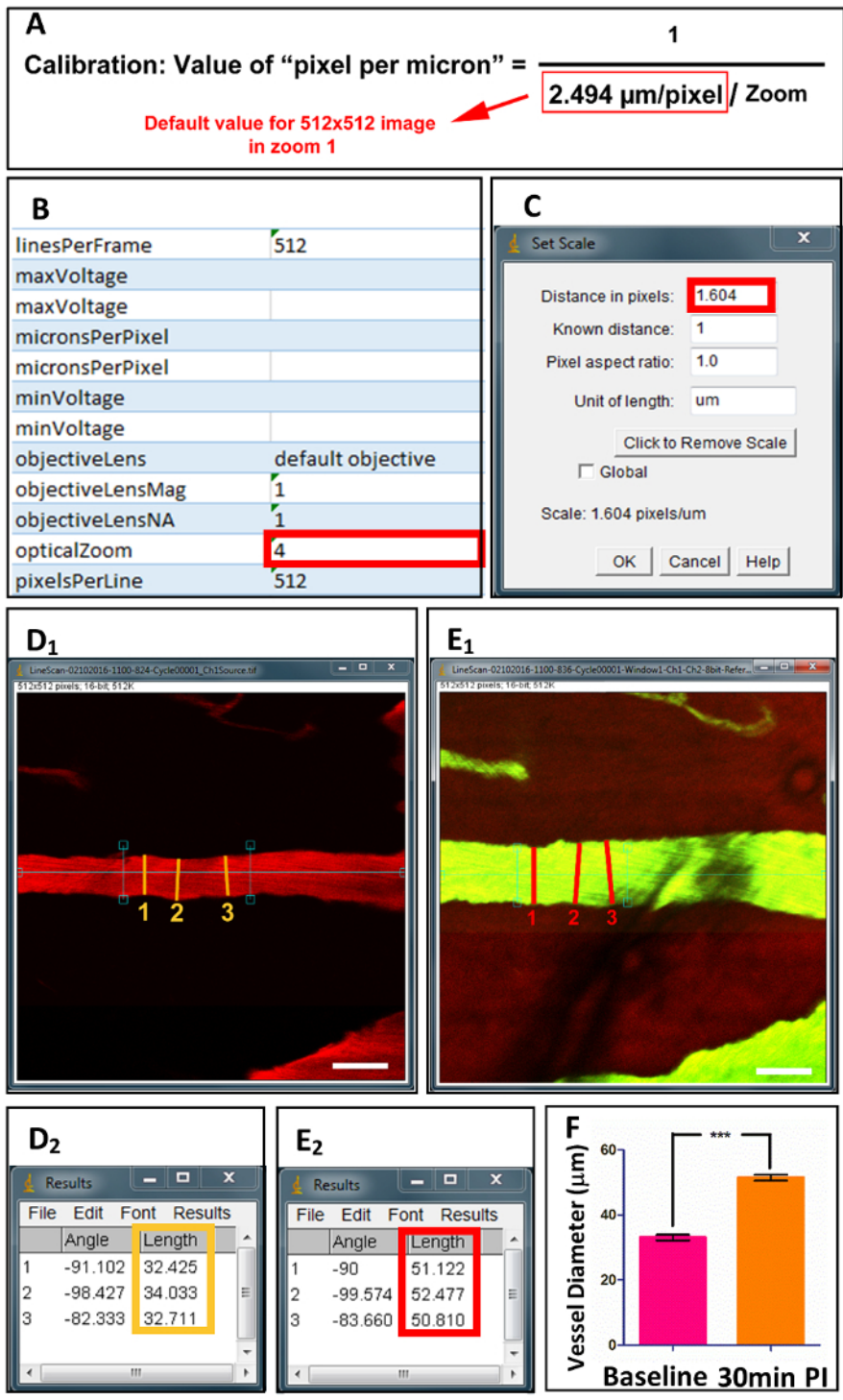
Figure 4. Acquisition and quantification of spinal vessel diameters.
Following preparation, single image files are acquired under 2P microscopy, along with XML files of calibrated values **(B)**. **(A)** The equation displays the calculation of "pixel per micron" based on optical zoom values. After calibration in ImageJ **(C)**, vessel diameters are measured at 3 points across the longitudinal axis before **(D₁)** and after **(E₁)** injury. **(D₂)** and **(E₂)** display the measured values. **(F)** Quantification of vessel diameters at baseline and 30 min post-injury. Scale bar = 50 µm. Data are shown as mean ± SD, ***p<0.0001, two-tailed paired t test. Please click here to view a larger version of this figure.
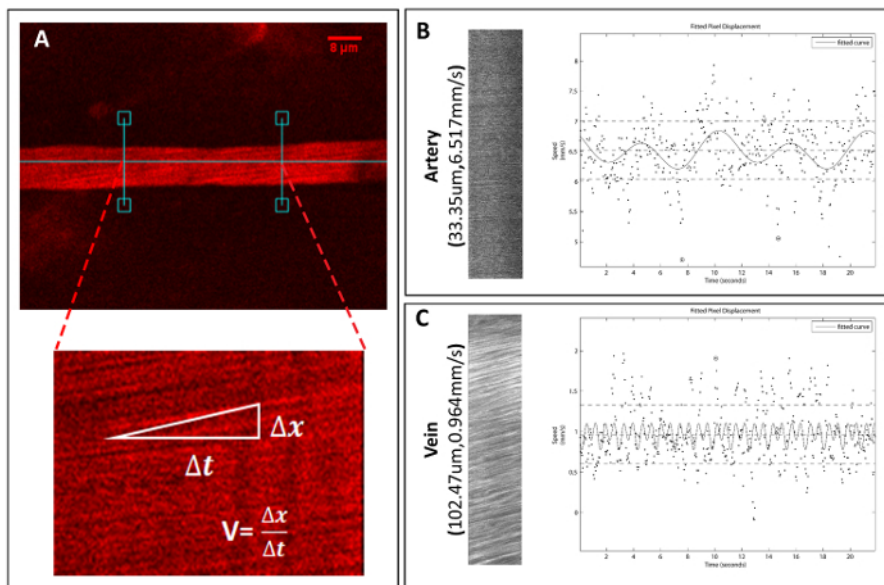
Figure 5. Acquisition and quantification of spinal vessel velocity.
Line-scan image files are acquired under 2P microscopy to calculate single vessel velocities. **(A)** An example of a selected vessel and method to assess blood vessel RBC velocity. **(B)** An arterial example of line-scan image and corresponding plot file for calculation of velocity, as well as an example of a vein **(C)**. Please click here to view a larger version of this figure.

	Artery	Vein
Morphology	Straight, smooth, thick vessel wall	Branches, rough edges
Blood Flow Velocity	Fast	Slow but varies
Diameter	30-80 μm	100-250 μm

Table 1: Criteria for Identifying Vessel Types

Discussion

One challenge for vascular studies following SCI is the technical limitation because traditional techniques are largely restricted to vascular structure changes in postmortem samples. This novel *in vivo* imaging method described above enables dynamic measurement of blood flow and related parameters (velocity and vessel diameter) using 2P-LSM in live rats. It also allows repeated examination in the same sets of vessels at different time points following contusive SCI. Previous 2-photon microscopy imaging techniques were unable to capture post-trauma vascular structures due to the leakage of a single tracer. Our duo-color design enables dynamic vascular imaging for traumatic models. In addition, the flexibility of this method provides an opportunity to generate a temporal-spatial profile of acute vascular changes following SCI.

There are several critical steps in our *in vivo* duo-color imaging method. First, it is fundamental to ensure the physical stability of spinal cord prior to time-lapse imaging, particularly reducing breathing motion artifact. We designed the shape of spinal clamps to raise the height of spinal vertebra slightly during stabilization. Thus the movement of spinal cord correlating to the breathing animal can be greatly reduced (**Figure 1D-F**, **2B**). It is recommended to check the stability of spinal cord prior to the beginning of each imaging session. If the spinal cord fails to achieve stability, the adjustment should be made to the alignment and tightness of spinal cord clamps. Second, peripheral tissue (bone, muscle layer, and skin) bleeding into the imaging window could risk contamination of the view. For a smooth imaging session, gelfoam and tissue adhesive glue should be applied to the surrounding tissue for effective prevention. Third, the fluorescent dyes we choose have a similar size as albumin (66 kDa), which is the main high molecular weight blood plasma protein. Under homeostatic conditions, the dyes were largely retained inside the vessel similar as albumin[28]. After the injury, the dyes passed through the disrupted endothelial structure and leaked into the parenchyma, causing a significant increased fluorescent intensity in the peripheral area of the vasculature (**Figure 3F-G**). In addition, there are two reasons why we choose external jugular vein catheterization. First, it can provide a consistently accessible route of delivery at any time of the experiment. Second, it can be used as a route for future treatment injection.

Although our *in vivo* duo-color method is able to provide a novel venue for traumatic vascular imaging studies, some caveats regarding this technique must be addressed. Currently, this technique is designed to assess vascular changes at 2 time points (baseline and 1 post-injury time point), but it is feasible to switch to multiple time points if additional fluorescent dyes and channels are available. Although there are several studies using implanted glass window for chronic intravital imaging, none of them can provide baseline information on the same vessel after traumatic injury[19,29,30,31,32]. Unlike these studies, our window is a no-glass window. This is convenient for pre- and post-injury imaging, but it may be challenging for re-establishing the window for long-term observation. Our future research is working on the technical improvement for chronic imaging. The vascular system is composed of several vessel types (artery, vein, and capillary) and each is different in aspects of morphology and function. Differentiation among vessel types during imaging could help to tease out a clear pattern of vascular changes. The protocol above depends on the observer identifying the vessels based on morphology and velocity; however, an artery-specific dye can be easily added to give a more definitive classification between vessel types[33].

This technique is not only limited to assessments on contusive and other traumatic models, such as crush injury and radiation injury, but also on studies focusing on disruption of BSCB, as well as vascular permeability changes. Besides SCI, it could be used to study the vascular changes following other neurodegenerative diseases such as amyotrophic lateral sclerosis (ALS) and multiple sclerosis (MS). Furthermore, it could be transferrable to a transgenic animal model to study the dynamic neurovascular interaction. As a powerful screening tool, future studies could utilize the imaging technique described here to assess the efficacy of treatment for spinal cord injury.

In conclusion, *in vivo* duo-color method is a reliable, real-time, *in vivo* approach tool for assessing dynamic vascular changes, which is ideal for characterization of temporal-spatial vascular profile and screening for treatments to reduce secondary damages following SCI.

Disclosures

The authors have nothing to disclose.

Acknowledgements

References

1. National Spinal Cord Injury Statistical Center. Spinal Cord Injury Facts and Figures at a Glance. *SCI Data Sheet 2016.* (2016).
2. Dumont, R. J. *et al.* Acute spinal cord injury, part I: pathophysiologic mechanisms. *Clin Neuropharmacol.* **24** (5), 254-264 (2001).
3. Beattie, M. S., Farooqui, A. A., & Bresnahan, J. C. Review of current evidence for apoptosis after spinal cord injury. *J Neurotrauma.* **17** (10), 915-925 (2000).
4. Liu, N. K. *et al.* A novel role of phospholipase A2 in mediating spinal cord secondary injury. *Ann Neurol.* **59** (4), 606-619 (2006).
5. Wu, X., & Xu, X. M. RhoA/Rho kinase in spinal cord injury. *Neural Regen Res.* **11** (1), 23-27 (2016).
6. Li, X. G. *et al.* Combination of methylprednisolone and rosiglitazone promotes recovery of neurological function after spinal cord injury. *Neural Regen Res.* **11** (10), 1678-1684 (2016).
7. Kulkarni, M. V. *et al.* Acute spinal cord injury: MR imaging at 1.5 T. *Radiology.* **164** (3), 837-843 (1987).
8. Tator, C. H., & Koyanagi, I. Vascular mechanisms in the pathophysiology of human spinal cord injury. *J Neurosurg.* **86** (3), 483-492 (1997).
9. Kobrine, A. I., Doyle, T. F., & Martins, A. N. Spinal cord blood flow in the rhesus monkey by the hydrogen clearance method. *Surg Neurol.* **2** (3), 197-200 (1974).
10. Rivlin, A. S., & Tator, C. H. Regional spinal cord blood flow in rats after severe cord trauma. *J Neurosurg.* **49** (6), 844-853 (1978).
11. Koyanagi, I., Tator, C. H., & Theriault, E. Silicone rubber microangiography of acute spinal cord injury in the rat. *Neurosurgery.* **32** (2), 260-268; discussion 268 (1993).
12. Noble, L. J., & Wrathall, J. R. Correlative analyses of lesion development and functional status after graded spinal cord contusive injuries in the rat. *Exp Neurol.* **103** (1), 34-40 (1989).
13. Maikos, J. T., & Shreiber, D. I. Immediate damage to the blood-spinal cord barrier due to mechanical trauma. *J Neurotrauma.* **24** (3), 492-507 (2007).
14. Tei, R., Kaido, T., Nakase, H., & Sakaki, T. Secondary spinal cord hypoperfusion of circumscribed areas after injury in rats. *Neurol Res.* **27** (4), 403-408 (2005).
15. Cohen, D. M. *et al.* Blood-spinal cord barrier permeability in experimental spinal cord injury: dynamic contrast-enhanced MRI. *NMR Biomed.* **22** (3), 332-341 (2009).
16. Drew, P. J., Shih, A. Y., & Kleinfeld, D. Fluctuating and sensory-induced vasodynamics in rodent cortex extend arteriole capacity. *Proc Natl Acad Sci U S A.* **108** (20), 8473-8478 (2011).
17. Schaffer, C. B. *et al.* Two-photon imaging of cortical surface microvessels reveals a robust redistribution in blood flow after vascular occlusion. *PLoS Biol.* **4** (2), e22 (2006).
18. Kim, T. N. *et al.* Line-scanning particle image velocimetry: an optical approach for quantifying a wide range of blood flow speeds in live animals. *PLoS One.* **7** (6), e38590 (2012).
19. Tang, P. *et al.* In vivo two-photon imaging of axonal dieback, blood flow, and calcium influx with methylprednisolone therapy after spinal cord injury. *Sci Rep.* **5** 9691 (2015).
20. Thrivikraman, K. V., Huot, R. L., & Plotsky, P. M. Jugular vein catheterization for repeated blood sampling in the unrestrained conscious rat. *Brain Res Brain Res Protoc.* **10** (2), 84-94 (2002).
21. Walker, M. J. *et al.* A novel vertebral stabilization method for producing contusive spinal cord injury. *J Vis Exp.* (95), e50149 (2015).
22. Anderson, K. D., Sharp, K. G., & Steward, O. Bilateral cervical contusion spinal cord injury in rats. *Exp Neurol.* **220** (1), 9-22 (2009).
23. Krishna, V. *et al.* A contusion model of severe spinal cord injury in rats. *J Vis Exp.* (78) (2013).
24. Lepore, A. C. Intraspinal cell transplantation for targeting cervical ventral horn in amyotrophic lateral sclerosis and traumatic spinal cord injury. *J Vis Exp.* (55) (2011).
25. Zhang, Y. P. *et al.* Spinal cord contusion based on precise vertebral stabilization and tissue displacement measured by combined assessment to discriminate small functional differences. *J Neurotrauma.* **25** (10), 1227-1240 (2008).
26. Wu, X. *et al.* A Tissue Displacement-based Contusive Spinal Cord Injury Model in Mice. *J Vis Exp.* (124) (2017).
27. Gage, G. J., Kipke, D. R., & Shain, W. Whole animal perfusion fixation for rodents. *J Vis Exp.* (65) (2012).
28. Egawa, G. *et al.* Intravital analysis of vascular permeability in mice using two-photon microscopy. *Sci Rep.* **3** 1932 (2013).
29. Farrar, M. J. *et al.* Chronic in vivo imaging in the mouse spinal cord using an implanted chamber. *Nat Methods.* **9** (3), 297-302 (2012).
30. Evans, T. A., Barkauskas, D. S., Myers, J. T., & Huang, A. Y. Intravital imaging of axonal interactions with microglia and macrophages in a mouse dorsal column crush injury. *J Vis Exp.* (93), e52228 (2014).

31. Davalos, D., & Akassoglou, K. In vivo imaging of the mouse spinal cord using two-photon microscopy. *J Vis Exp.* (59), e2760 (2012).
32. Davalos, D. *et al.* Stable in vivo imaging of densely populated glia, axons and blood vessels in the mouse spinal cord using two-photon microscopy. *J Neurosci Methods.* **169** (1), 1-7 (2008).
33. Shen, Z., Lu, Z., Chhatbar, P. Y., O'Herron, P., & Kara, P. An artery-specific fluorescent dye for studying neurovascular coupling. *Nat Methods.* **9** (3), 273-276 (2012).